OPEN ACCESS
IOP Publishing | Institute of Physics and Engineering in Medicine Physics in Medicine & Biology
Phys. Med. Biol. **61** (2016) 4438–4451 doi:10.1088/0031-9155/61/12/4438

Simple estimation of induced electric fields in nervous system tissues for human exposure to non-uniform electric fields at power frequency

Hiroo Tarao[1,5], Hironobu Miyamoto[1], Leena Korpinen[2], Noriyuki Hayashi[3] and Katsuo Isaka[4]

[1] National Institute of Technology, Kagawa College, 355 Chokushi-cho, Takamatsu, Kagawa 761-8058, Japan
[2] Tampere University of Technology, Tampere, Finland
[3] University of Miyazaki, Miyazaki, Japan
[4] The University of Tokushima, Tokushima, Japan

E-mail: tarao@t.kagawa-nct.ac.jp

Received 11 November 2015, revised 6 January 2016
Accepted for publication 4 February 2016
Published 25 May 2016

Abstract

Most results regarding induced current in the human body related to electric field dosimetry have been calculated under uniform field conditions. We have found in previous work that a contact current is a more suitable way to evaluate induced electric fields, even in the case of exposure to non-uniform fields. If the relationship between induced currents and external non-uniform fields can be understood, induced electric fields in nervous system tissues may be able to be estimated from measurements of ambient non-uniform fields. In the present paper, we numerically calculated the induced electric fields and currents in a human model by considering non-uniform fields based on distortion by a cubic conductor under an unperturbed electric field of 1 kV m^{-1} at 60 Hz. We investigated the relationship between a non-uniform external electric field with no human present and the induced current through the neck, and the relationship between the current through the neck and the induced electric fields in nervous system tissues such as the brain, heart, and spinal cord. The results showed that the current through the neck can be formulated

[5] Author to whom any correspondence should be addressed.

by means of an external electric field at the central position of the human head, and the distance between the conductor and the human model. As expected, there is a strong correlation between the current through the neck and the induced electric fields in the nervous system tissues. The combination of these relationships indicates that induced electric fields in these tissues can be estimated solely by measurements of the external field at a point and the distance from the conductor.

Keywords: numerical human model, cubic conductor, induced current through the neck, brain, spinal cord

(Some figures may appear in colour only in the online journal)

1. Introduction

Stimulations based on currents induced in the human body by extremely low frequency (ELF) electric and magnetic fields can be regarded as a factor in adverse health effects in humans. Accordingly, induced currents in a numerical human body model from electric and magnetic fields have been calculated in several previous studies (Dawson *et al* 1998, Dawson and Stuchly 1998, Dimbylow 1998, Dimbylow 2000, Stuchly and Dawson 2002, Leitgeb and Cech 2008). Most results were calculated under uniform fields, with very few results under realistic non-uniform magnetic fields, such as those in a substation and from home appliances (Cheng *et al* 1995, Dawson *et al* 1999, Gandhi *et al* 2001). In the case of magnetic field exposure, estimations of induced currents in a spherical model or a human model by non-uniform magnetic fields that are produced by currents from single and double wires were carried out (IEC 2004a, Yamazaki *et al* 2005, 2007). In the IEC 62226-2-1, the coupling factors for non-uniform magnetic fields for several different types of magnetic sources are indicated. In addition, understanding of magnetic field exposure has been advanced by a number of numerically dosimetric studies, including studies using models of specific tissues such as the retina and skin (Hirata *et al* 2011, Santis *et al* 2016, Schmid and Hirtl 2016).

In the case of electric field exposure, meanwhile, induced electric fields in a spheroid model in a uniform electric field were theoretically derived (Shiau and Valentino 1981). Also, currents induced in both ankles of a grounded human body were measured and formulated (Deno and Zaffanella 1982). These calculated results (i.e. short circuit currents) are consistent with numerically calculated results using anatomical human models that have often been used recently (Dawson *et al* 1998, Tarao *et al* 2013). However, these calculations do not consider non-uniform field exposure, which is unrealistic because electric fields are readily perturbed by a conductor. In the IEC 62226-3-1 (2004b), methods to calculate currents induced by electric field exposures are described, but non-uniform field exposures are not covered.

Experimental data concerning external electric fields in substations and induced currents through the necks of workers were reported (Korpinen *et al* 2009, 2012), and the results showed that there is a rough correlation between them. Furthermore, in our previous work we found that a contact current or a short circuit current is a more suitable factor for evaluating induced electric fields, even in the case of a non-uniform field exposure (Tarao *et al* 2013). Therefore, if the relationship between ambient non-uniform electric fields and induced currents in the body can be made clear, induced electric fields in nervous system tissues such as the brain and spinal cord could possibly be estimated by measuring ambient non-uniform electric fields.

In the present paper, in relation to the electrical safety of workers in substations, our goal is to develop an estimation technique for induced electric fields in the nervous system tissues

of workers based on measurements of ambient external electric fields. The EU Directive 2013/35/EU, which is intended to improve regulations for workplace safety, seeks to limit workers' exposure to electric and magnetic fields. EU member nations must apply it by July 2016 (The European Parliament and the Council of the European Union 2013). Thus, there is a clear need for a practical method of estimating induced electric fields for these workers.

First, we numerically calculated the induced currents in a human model by considering a non-uniform electric field that is distorted by a cubic conductive object, which assumes a grounded metal structure in a substation, under an unperturbed electric field at power frequency. In the calculations, the height of the conductive object and the distance between the human model and the object are varied to consider the different types of non-uniformity. Then, from the calculated results, we examined the relationship between the external electric field and the induced current through the neck of the model. We have a good record of using a current through the neck, and we confirmed that the induced electric fields in the nervous system tissues of the model correlate with the currents through the neck. Finally, we investigated an approximate expression to obtain induced electric fields in those tissues from experimental measurements of ambient non-uniform electric fields.

2. Numerical procedures

2.1. Numerical method

Electric fields and currents induced in a voxelized human model exposed to ELF external electric fields were calculated based on the scalar potential finite difference (SPFD) method (Dimbylow 1998). This method was originally used for low-frequency induction by magnetic fields, but has been improved for use with electric field exposure. In the case of the SPFD method of magnetic induction, only the region inside a numerical human model is required as the computational domain. However, in the case of the improved method for electric field exposure, the computational domain includes a large region outside the human model as well as the region inside the human model. Therefore, this numerical computation for electric field exposures using the improved method requires very large nodes. A detailed description of the numerical method and its validation is available from Tarao *et al* (2013).

2.2. Human model

A realistic human model of an adult male (Duke), 1.80 m in height, comprising 77 tissues and organs, was used for the numerical calculations (Christ *et al* 2010). The model has a bounding box of 0.61 m $\times$ 0.31 m $\times$ 1.86 m for the x-, y-, and z-axes, respectively. The voxel size of the model can be adjusted from 0.1 mm to a maximum of 5 mm. Selecting the maximum size results in approximately 2.8 million voxels for the bounding box itself. This size was selected for the present study, because in our case we had to locate the model within a much larger computational area (discussed in the next section). The typical conductivity values at power frequency corresponding to particular tissues were used based on the measurements reported by Gabriel *et al* (1996, 2009) and were assigned to each voxel of the numerical model.

2.3. Exposure condition

The entire computational domain used in the study was a cubic space with dimensions 20 m $\times$ 10 m $\times$ 16 m for the x-, y-, and z-axes, respectively. A high potential electrode (16 kV) on the top surface of the domain and a ground electrode on the bottom surface of the domain

were attached to generate a vertical uniform electric field of 1 kV m^{-1} at 60 Hz in the computational domain. The numerical human model (Duke) stood on the center of the ground plane and was grounded. A conductive object with dimensions 0.5 m × 0.5 m for the *x*- and *y*-axes, which was also grounded, was placed in front of the human model so that the human model would encounter non-uniform electric fields that were distorted by the object. As illustrated in figure 1, the height of the object (h) varied from 2 m up to 5 m, and the distance (d) between the surface of the object and the center axis of the human model also varied from 0.25 m up to 4 m, to produce different types of non-uniformity around the object. The computational domain was divided into various voxel sizes, ranging from 5 mm for the bounding box of the numerical human model to 1.28 m for the edge of the domain. The selected sizes reduced the total number of voxels to about 20 million.

After the numerical calculations were performed by varying the height (h) of the conductive object and the distance (d) from the object, the relationship between the ambient external electric fields and the induced currents flowing through the neck of the human model, and the relationship between the induced currents in the neck and the induced electric fields in the nervous system tissues (i.e. the brain, heart, nerves, and spinal cord) of the human model were investigated. Here, the external field is defined as the electric field strength (E_{ext}) at the central position of the numerical human head (1.7 m height from the ground) with no human present (see figure 1), since currents induced in the neck are caused by potential differences based on the electrification charges on the human head.

3. Results and discussion

3.1. External electric field and its non-uniformity

Figure 1 shows the distribution of the equipotential line and electric field vector around the conductive object with no human present. It is clear from the figure that the electric field around the object is distorted and becomes non-uniform. In the IEC 62110 (2009), the non-uniformity of electric fields (E_{NU}) is defined as,

$$E_{NU} = \left|E_{1.5} - E_{avg}\right| / E_{avg} \times 100\% \tag{1}$$

where $E_{1.5}$ is the electric field strength at 1.5 m above the ground, which is the value at the largest difference in the numerator, and E_{avg} is the electric field level at heights of 0.5 m, 1.0 mm, and 1.5 m above the ground. Table 1 indicates the electric field strengths calculated with no human present and the averaged value (E_{avg}), which also shows the non-uniformity (E_{NU}). In the table, the electric fields at a point 1.5 m near the object exceed 1 kV m^{-1}. For example, the electric field strengths at 1.5 m for $h = 2$ m are 1.7 kV m^{-1}, 1.3 kV m^{-1}, and 1.1 kV m^{-1} for $d = 0.25$ m, 0.45 m, and 0.65 m, respectively, where the non-uniformity ranges from 30% to 55%. In contrast, the non-uniformity reduces by a small percentage 2 m from the object, becoming more uniform. Only a few measured non-uniform electric fields related to the non-uniformity were reported, because electric field meters are generally calibrated under a uniform field. One example is the measurement of electric fields in a corridor of an EHV substation (Deno and Zaffanella 1982). The measured data were 3.7, 4.43, and 6.7 kV m^{-1} at 0.5, 1.0, and 2.0 m above the ground, respectively. In this case, the non-uniformity was 35.5%; however, note that the highest measured point was not 1.5 m. Therefore, the range of the non-uniformity investigated in the present study covers a practical situation encountered in a substation.

Figure 2 shows the calculated results of both the equipotential line and electric field vector around the human model for the different distances from the surface of the object. It can be

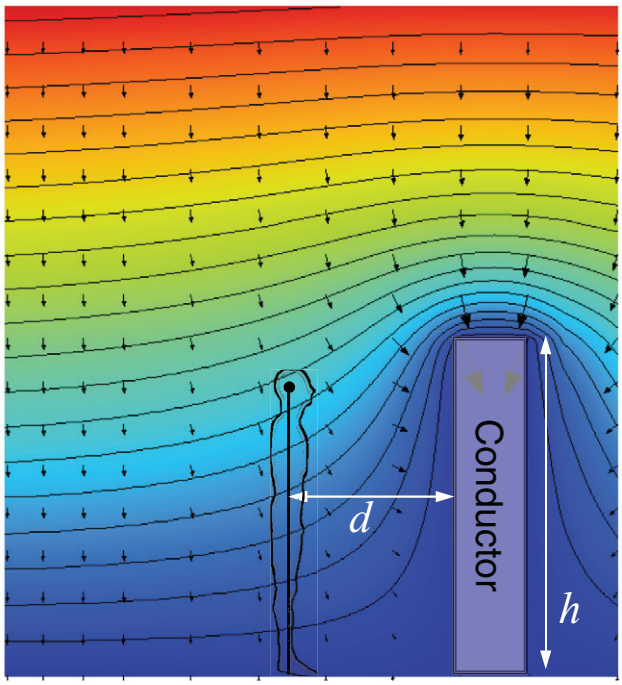

Figure 1. Distribution of equipotential line and external electric field around the conductive object, with no human present under a uniform electric field of 1 kV m^{-1} at 60 Hz. The equipotential line is represented at 200 V intervals. Both widths of the object are 0.5 m, and the height (h) is 2 m. The external electric field is defined as the field at the central position of the numerical human head (i.e. 1.7 m height from the ground), with no human present, to give an indication of non-uniform fields.

seen from figure 2 that the electric field interacting with the human body (in particular, the frontal side of the human) decreases with a closer approach to the conductive object because of the existence of the object. This results in the induced current through the human body also decreasing.

3.2. Currents through the neck

Figure 3 shows the induced current flowing downward, perpendicular to each horizontal layer of the human body for the different distances from the surface of the conductive object. From the figure, the induced current through the neck in the case of a uniform field of 1 kV m^{-1} at 60 Hz is 5 μA, which is about 27% of the total current through the ankles (i.e. short circuit current). The induced current decreases as the distance from the object decreases, since the electric field getting through the human body decreases, as expected.

Figure 4 shows the induced current through the neck of the human model as a function of the external field (E_{ext}) for the different h and d. The straight line in the figure represents the current through the neck in the case of a uniform electric field, which is based on the fact that the current value in the neck for the uniform field exposure shown in figure 3, as expressed by:

$$I_{neck} = 5\times 10^{-9} \times E_{uni} \times (f/60) \quad \text{(A)} \tag{2}$$

Table 1. Calculated electric field strength, its averaged value, and the non-uniformity with no human present for the different heights of the conductive object and the different distances from the object.

		Electric field above the ground (kV m^{-1})				
h (m)	d (m)	0.5 m	1.0 m	1.5 m	E_{avg} (kV m^{-1})	E_{NU} (%)
2	0.25	0.554	1.039	1.697	1.097	54.7
	0.45	0.566	0.874	1.300	0.914	42.3
	0.65	0.627	0.823	1.109	0.853	30.0
	0.85	0.688	0.822	1.017	0.842	20.7
	1.15	0.767	0.849	0.968	0.861	12.4
	2.15	0.905	0.927	0.957	0.930	2.9
	4.14	0.971	0.974	0.979	0.930	0.5
5	0.25	0.326	0.590	0.865	0.594	45.7
	0.45	0.338	0.500	0.690	0.509	35.4
	0.65	0.378	0.477	0.609	0.488	24.8
	0.85	0.421	0.485	0.576	0.494	16.6
	1.15	0.483	0.520	0.577	0.527	9.6
	2.15	0.630	0.642	0.662	0.645	2.7
	3.15	0.709	0.717	0.728	0.718	1.4

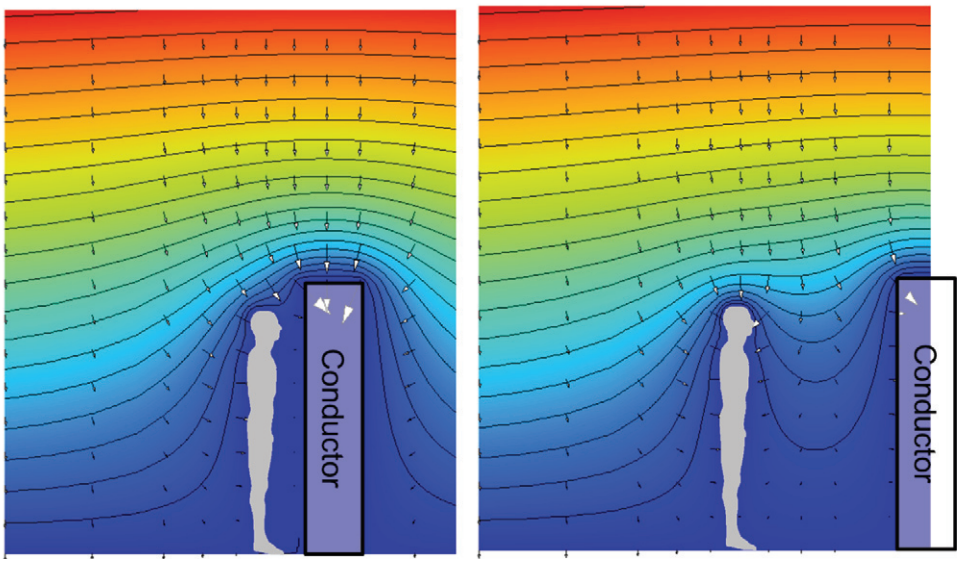

Figure 2. Distribution of the equipotential line and external electric field around the conductive object when the numerical human model stands erect (a) $d = 0.25$ m and (b) $d = 1.15$ m from the surface of the object. The height of the object is 2 m. The external electric field is a uniform field of 1 kV m^{-1} at 60 Hz. The equipotential line is represented at 200 V intervals.

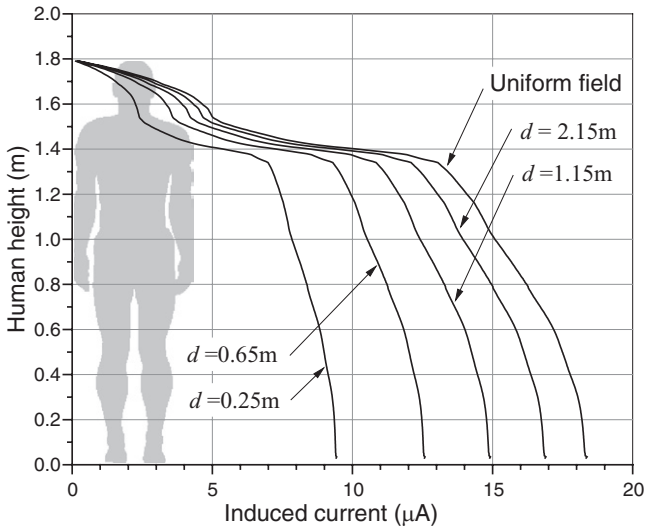

Figure 3. Current through the horizontal layer along the human body for the different distances (d) from the surface of the conductive object. The height of the object is 2 m.

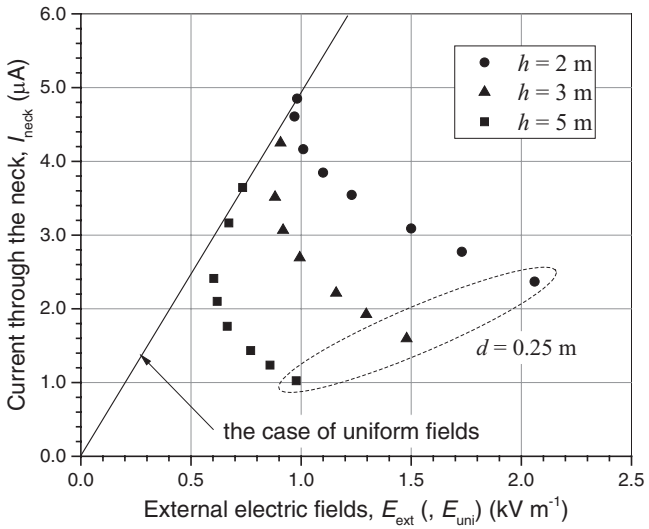

Figure 4. Current through the neck (I_{neck}) for the different heights of the object (h) and the different distances from the object (d) as a function of the external electric field (E_{ext}). The straight line represents the case of a uniform field exposure, as indicated in equation (2).

where E_{uni} is the external electric field strength for a uniform exposure and f is the frequency. In the case of an electric field exposure at low frequency, induced electric fields and currents in the body are proportional to the frequency as the complex conductivity outside the body (i.e. air) can be regarded as $\omega\varepsilon_0$, and its magnitude is very small compared with the magnitude of the complex conductivity inside the body (Shiau and Valentino 1981, Kaune *et al* 1997). As indicated in figure 4, all the plots stay below the straight line, even when the point electric field at 1.7 m above the ground exceeds 1 kV m^{-1}, and show a non-linear relationship against E_{ext}.

The currents through the neck decrease non-linearly as the body moves closer to the object for any object height, since the electric potentials at the head position (but with no human present) decrease (see figure 1). In contrast, the plots coincide with the case of a uniform field exposure when the distance (d) is large. External electric fields around power equipment in 400 kV substations and currents in the heads of workers during their maintenance were previously measured (Korpinen *et al* 2009, 2012). The results showed that there was a rough correlation between the current through the neck and the external field at 1.7 m above the ground, but the distance from the equipment is not completely described. Consequently, all data regarding current through the neck, as indicated in the literature, seem to be lower than those obtained from equation (2), which shows a similar tendency to figure 4.

Figure 5 shows the ratio of the current through the neck (I_{neck}) under non-uniform exposure with E_{ext} to another current through the neck by a uniform field with strength equal to E_{ext}, as a function of distance (d). For a distance greater than about 4 m, the ratio reaches 100%, so it can be regarded as a uniform field. In contrast, for distances below 4 m, the ratio depends only on the distance. Using curve fitting based on the calculated results, the reduction rate can be expressed by:

$$K_{\mathrm{I}} = (1-1.16\mathrm{e}^{-1.5d}) \times 100\% \tag{3}$$

which is shown in figure 5 and demonstrates that the reduction rate can be determined by the distance from the object, regardless of the height. In equation (3), K_{I} becomes zero if d is about 0.1 m, which is the situation in which the largest area of the human body contacts the conductive object, and which is not covered in this study. For $d = 0.45$ m and $h = 2$ m, K_{I} is 40.9% from equation (3). Because the external field strength and the current in the neck were 1.5 kV m^{-1} and 3.09 μA, respectively, K_{I} can be estimated as 41.2% with a current of 7.5 μA in the neck for uniform exposure taken into consideration. Therefore, these reduction rates are in excellent agreement with each other.

3.3. Induced electric fields in nervous system tissues

Figure 6 shows the 99th percentile values of the induced electric fields (E_{tissue}), which are based on the International Commission on Non-Ionizing Radiation Protection (ICNIRP) guidelines (2010), in the brain, heart, peripheral nerves, and spinal cord against the current through the neck (I_{neck}). It is clear from figure 6 that the induced electric fields in these nervous system tissues are strongly correlated with the induced currents through the neck under all conditions, as predicted by previous work (Tarao *et al* 2013), which indicates that these induced electric fields can be estimated from the currents through the neck, expressed approximately by:

$$E_{\mathrm{tissue}} = K_{\mathrm{tissue}} \times I_{\mathrm{neck}} \quad (\mathrm{V\,m^{-1}}) \tag{4}$$

where K_{tissue} is the slope of the straight line shown in figure 6, as indicated in table 2. From the calculation for $d = 0.45$ m and $h = 2$ m, the current in the neck and induced electric field in the brain were 3.09 μA and 1.64 mV m^{-1}, respectively. Therefore, the slope can be estimated as 530.7, with an error of 5.8%. Korpinen *et al* (2012) tabulated induced electric fields in the head estimated by measurements of currents through the necks of humans working in substations. This induced field was calculated by dividing averaged current density in the neck by a conductivity of 0.1–0.2 S m^{-1}, which are typical values of tissue conductivity. These induced electric fields are comparable with the values obtained from equation (4).

Figure 7 shows an example of the induced electric field distribution on the horizontal cross-section, including the brain of the human model, for the different distances from the object. It can be seen that the induced electric fields in the tissues existing between the skull and skin,

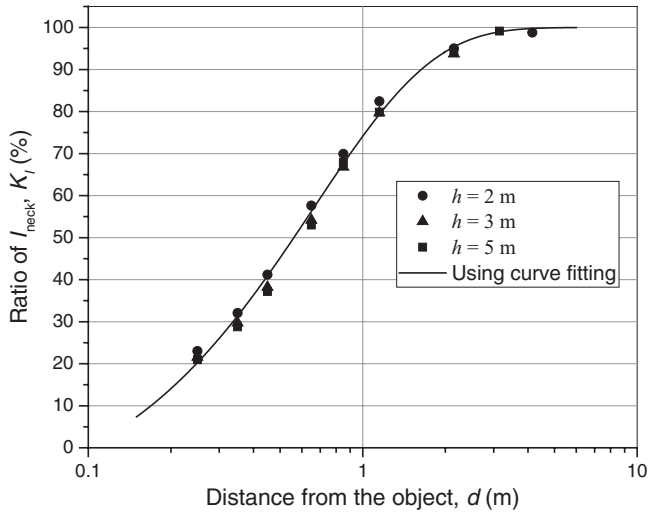

Figure 5. The ratio (K_I) of the current through the neck (I_{neck}) in the case of the external electric field (E_{ext}) to another I_{neck} by a uniform field equivalent to the E_{ext}, as a function of the distance (d) from the surface of the object.

such as subcutaneous adipose tissues, are higher than those in the brain. In particular, the induced fields in the frontal side of the head increase as the distance increases, as is obvious from figure 2. The vectors in figure 7 are all unit vectors. However, the lengths of the vectors in the brain seem to be somewhat shorter, which means that the vertical component of the induced fields is dominant.

3.4. Estimation of induced field by measuring the external field

By combining equations (2)–(4), the approximated E_{tissue} can be derived by:

$$E_{tissue} = 5\times 10^{-9} \times K_{tissue} \times (1-1.16e^{-1.5d}) \times E_{ext} \times (f/60) \quad (V\,m^{-1}) \qquad (5)$$

In the proposed estimation, measurements of the external electric field at a point in the center of the human head and the distance from the conductive object are needed to obtain the maximum value of the induced electric fields in the nervous system tissues.

3.5. Validation

3.5.1. Ungrounded human. The calculations in the present paper were carried out with the numerical human model grounded. If an ungrounded human stands beside the conductive object, currents induced in the neck of the human body should be smaller than in the case of a grounded human. Therefore, the reduction rate should be smaller than that in the curve indicated in equation (3), which can be thought of as underestimation. However, if an ungrounded human touches a conductor, a contact current, which is the total current flowing out from the body to the ground, has the same value as in a short-circuit current from the feet of a grounded human (Tarao *et al* 2013), allowing the application of our method. In any case, the relationship between the current in the neck and the induced electric fields in the nervous system tissues does not change.

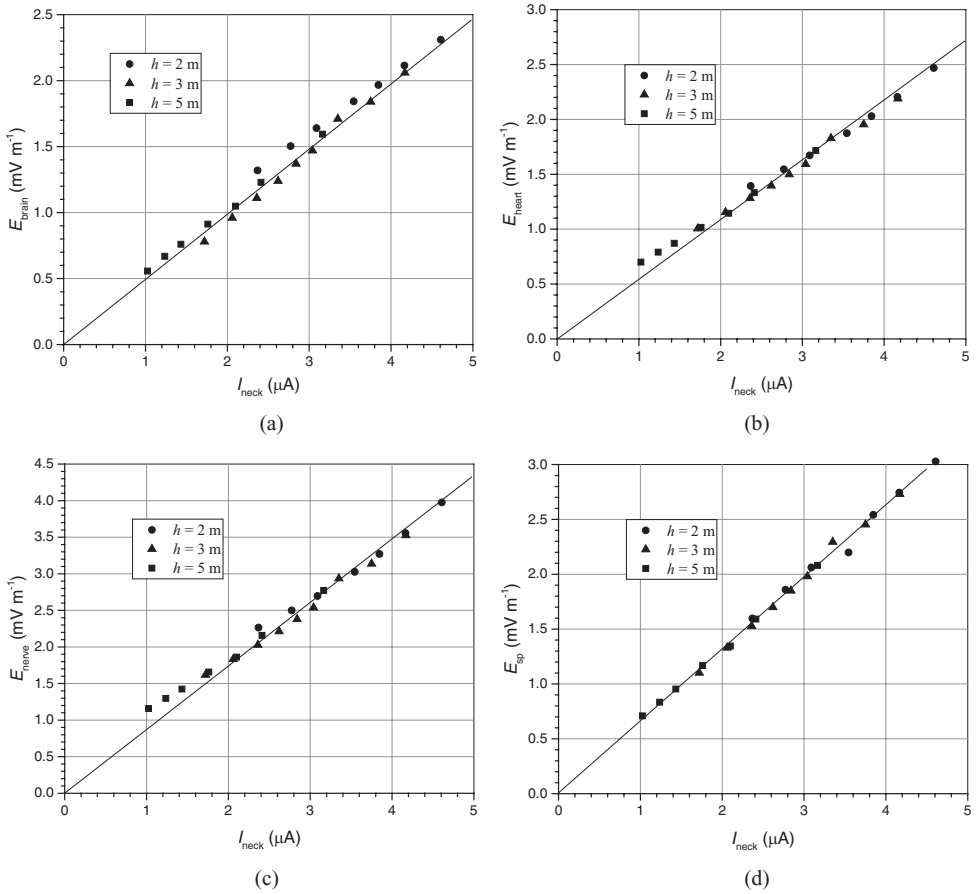

Figure 6. Induced electric field in the nervous system tissues against the current through the neck (I_{neck}) for non-uniform field exposures: (a) brain, (b) heart, (c) nerves, and (d) spinal cord. The slope of the straight line is indicated in table 2.

Table 2. Coefficient of the induced electric field in the given tissue to the current through the neck, as indicated in equation (4).

	Brain	Heart	Nerves	Spinal cord
K_{tissue} ((V m^{-1}) A^{-1})	500	540	880	660

3.5.2. 99th percentile value of induced field. According to the ICNIRP guidelines established in 2010 (ICNIRP 2010), the induced electric field to be compared with the basic restrictions is recommended as a vector average of the electric field in a small contiguous tissue volume of $2 \times 2 \times 2\,\text{mm}^3$, although we used a voxel size of 5 mm in the present study. The effects of averaging the volume of the voxels on induced electric fields in the brain of a numerical human model exposed to a uniform electric field were previously investigated (Hirata *et al* 2010). These authors concluded that the 99th percentile value of an electric field in nerve tissue is more stable than that of the maximal value for the different averaging volumes. Figure 8 shows the percentile values of the induced electric field in the nervous system tissues of a Duke model for a uniform electric field (1 kV m^{-1} at 60 Hz) with a voxel size of 2 mm

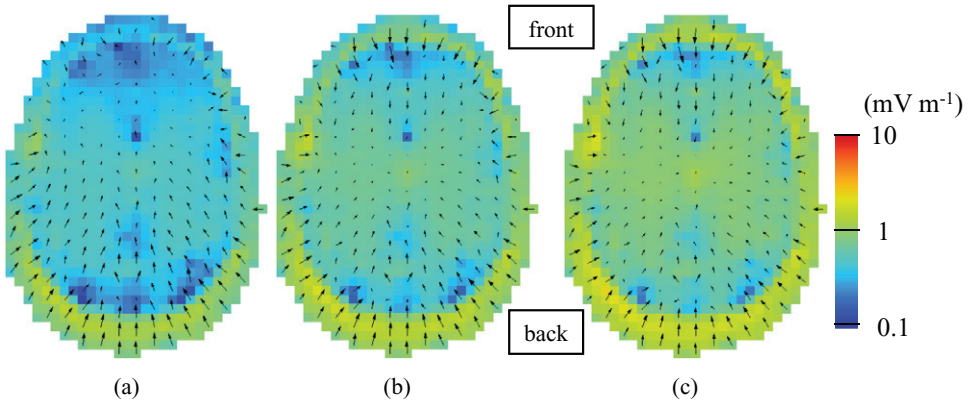

Figure 7. Induced electric field distribution on the horizontal cross-section including the brain of the human model for (a) $d = 0.25$ m, (b) $d = 0.65$ m, and (c) $d = 2.15$ m when the height of the object (h) is 2 m.

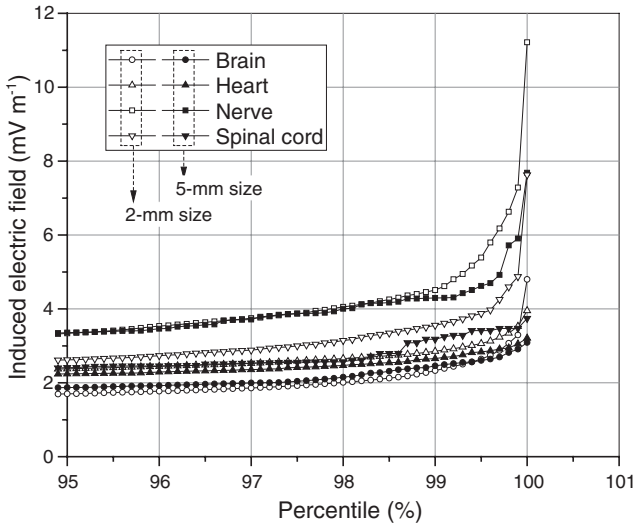

Figure 8. Percentile values of the induced electric field in the nervous system tissues for a uniform electric field exposure (1 kV m^{-1}, 60 Hz) with a voxel size of 2 mm (opened) and 5 mm (closed).

and 5 mm. The result in the case of a voxel size of 2 mm was obtained using a two-stage approach (Tarao *et al* 2013). It is noted that the currents induced through each horizontal cross-section of the body obtained from the numerical human models, such as in figure 3, with different voxel sizes are in agreement with each other. However, the induced electric fields differ depending on the voxel size as an electric field is a kind of density. It can be seen in figure 8 that the results obtained for the 2 mm and the 5 mm voxels were almost consistent up to about 99%, except for the spinal cord. The maximum value of the induced fields in the nerves can be observed to have a staircase error even for a voxel size of 5 mm. It has been reported that the 99th percentile value could significantly underestimate the actual induced field level (Chen *et al* 2013). Further work could be necessary to fully understand the maximum value.

Table 3. Electric field in the given tissues estimated from equation (5).

		Estimated electric field, E_{tissue} (mV m^{-1})			
d (m)	E_{ext} (kV m^{-1})	Brain	Heart	Nerves	Spinal cord
0.25	21.0	8.87 (11.4)	9.58 (11.8)	15.6 (18.9)	11.7 (15.4)
0.45	15.6	13.3 (13.4)	14.4 (14.5)	23.4 (23.1)	17.6 (19.0)
0.65	12.8	15.0 (14.6)	16.2 (16.4)	26.4 (26.0)	19.8 (21.3)

The value in parentheses shows the results from the previous work (Tarao *et al* 2013).

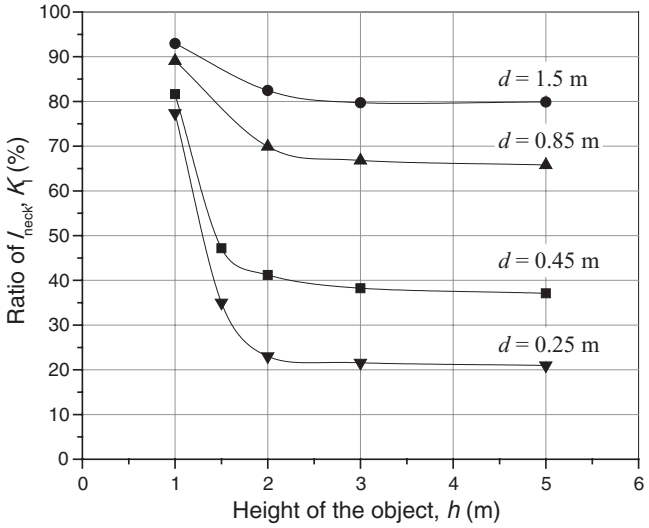

Figure 9. The reduction rate (K_I) of the current through the neck (I_{neck}) as a function of the height (h) of the conductive object.

3.5.3. Comparison with the previous report. We reported previously the induced currents and electric fields in a worker engaging in the maintenance of an operational circuit breaker in a substation, considering human exposure to a non-uniform electric field (Tarao *et al* 2013). In this case, the external electric fields at 1.7 m were 21.0, 15.6, and 12.8 kV m^{-1} at 50 Hz for the distances of 0.25, 0.45, and 0.65 m, respectively. It is noted that the distance is adapted to that defined in the present study. Substituting these values in equation (5), the induced electric fields in the tissues (E_{tissue}) can be calculated, as indicated in table 3. The estimated values are in greater agreement with the previous results shown in parentheses as the distance increases. In particular, in the case of a distance of 0.65 m, which is generally maintained in a substation, these values are in excellent agreement with each other.

3.5.4. Effect of conductor size. Finally, in the present calculations, a non-uniform electric field encountered in a substation was given by assuming a geometrically complex metal structure as the simply configured conductive object. The method presented here provides for estimating induced electric fields in various nervous system tissues of a worker near a conductive object with a certain width, as used in the present calculation. Assuming that the worker stands beside a metal pole in a substation, the reduction rate will exceed the upper bound indicated in equation (3) and figure 5, because the worker is exposed to more electric fields as they emanate from both sides of the pole. Also, figure 9 shows the reduction rate for the different

distances (d) from the object as a function of the height of the object. We found that the reduction rate increases sharply when the object height is below the human model height. This method has some room for improvement. However, even in such cases, the induced fields in the nervous system tissues correlated closely with the current through the neck.

4. Conclusion

In the present paper, to provide a simple method for the estimation of induced electric fields in the nervous system tissues of an adult human exposed to a non-uniform electric field, induced electric fields and currents in the numerical human model were examined under different types of non-uniformity.

As expected, induced currents through the neck of the model were non-linear to the external electric fields when there was no human present. However, the induced currents depend on the distance from the surface of the object, regardless of the height of the object considered, and can be approximately formulated. Meanwhile, we confirmed that there was a strong correlation between the induced current through the neck and the induced electric fields in the nervous system tissues in all conditions. Consequently, the combination of these findings facilitates the estimation of the induced electric fields in those tissues from the external electric field at the central position of the human head and the distance from the object, both of which can be readily measured. The present simple estimation method can be applied in limited cases, such as when a conductive object is a device or a piece of equipment with a certain width and is taller than a human's height. Further investigations of accounting for non-uniformity in estimation methods are needed to extend the coverage of the applicable conditions.

Acknowledgments

We would like to thank Dr K Yamazaki from the Central Research Institute of Electric Power Industry (CRIEPI), Japan, Professor M Taki from Tokyo Metropolitan University, and Professor O Fujiwara from Nagoya Institute of Technology for helpful advice in writing the present paper.

References

Chen X L, Benkler S, Chavannes N, Santis V D, Bakker J, Rhoon G, Mosig J and Kuster N 2013 Analysis of human brain exposure to low-frequency magnetic fields: a numerical assessment of spatially averaged electric fields and exposure limits *Bioelectromagnetics* **34** 375–84

Cheng J, Stuchly M A, DeWagter C and Nartens L 1995 Magnetic field induced currents in a human head from use of portable appliances *Phys. Med. Biol.* **40** 495–510

Christ A *et al* 2010 The virtual family—development of surface-based anatomical models of two adults and two children for dosimetric simulations *Phys. Med. Biol.* **55** N23–38

Dawson T W, Caputa K and Stuchly M A 1998 High-resolution organ dosimetry for human exposure to low-frequency electric fields *IEEE Trans. Power Deliv.* **13** 366–73

Dawson T W, Caputa C and Stuchly M A 1999 Numerical evaluation of 60 Hz magnetic induction in the human body in complex occupational environments *Phys. Med. Biol.* **44** 1025–40

Dawson T W and Stuchly M A 1998 High-resolution organ dosimetry for human exposure to low-frequency magnetic fields *IEEE Trans. Magn.* **34** 708–18

Deno D W and Zaffanella L E 1982 Field effects of overhead transmission lines and stations *Transmission Line Reference Book 345 kV and Above* 2nd edn (Palo Alto, CA: Electric Power Research Institute) pp 329–420

Dimbylow P J 1998 Induced current densities from low-frequency magnetic fields in a 2 mm resolution, anatomically realistic model of the body *Phys. Med. Biol.* **43** 221–30
Dimbylow P J 2000 Current densities in a 2 mm resolution anatomically realistic model of the body induced by low frequency electric fields *Phys. Med. Biol.* **45** 1013–22
Gabriel S, Lau R W and Gabriel C 1996 The dielectric properties of biological tissues: III. Parametric models for the dielectric spectrum of tissues *Phys. Med. Biol.* **41** 2271–93
Gabriel C, Peyman A and Grant E H 2009 Electrical conductivity of tissue at frequencies below 1 MHz *Phys. Med. Biol.* **54** 4863–78
Gandhi O P, Kang G and Wu D Lazzi G 2001 Currents induced in anatomic models of the human for uniform and nonuniform power frequency magnetic fields *Bioelectromagnetics* **22** 112–21
Hirata A, Takano Y, Fujiwara O, Dovan T and Kavet R 2011 An electric field induced in the retina and brain at threshold magnetic flux density causing magnetophosphenes *Phys. Med. Biol.* **56** 4091–101
Hirata A, Takano Y, Kamimura Y and Fujiwara O 2010 Effect of the averaging volume and algorithm on the *in situ* electric field for uniform electric- and magnetic-field exposures *Phys. Med. Biol.* **55** N243–52
ICNIRP (International Commission on Non-Ionizing Radiation Protection) 2010 Guidelines for limiting exposure to time-varying electric and magnetic fields (1 Hz–100 kHz) *Health Phys.* **99** 818–36
IEC (International Electrotechnical Commission) 2004a Exposure to electric or magnetic fields in the low and intermediate frequency range—methods for calculating the current density and internal electric field induced in the human body, part 2-1: exposure to magnetic fields—2D models IEC62226-2-1
IEC (International Electrotechnical Commission) 2004b Exposure to electric or magnetic fields in the low and intermediate frequency range—methods for calculating the current density and internal electric field induced in the human body, part 3-1: exposure to electric fields—analytical and 2D numerical models IEC62226-3-1
IEC (International Electrotechnical Commission) 2009 Electric and magnetic field levels generated by AC power systems—measurement procedures with regard to public exposure IEC 62110 Ed. 1.0
Kaune W T, Guttman J L and Kavet R 1997 Comparison of coupling of humans to electric and magnetic fields with frequencies between 100 Hz and 100 kHz *Bioelectromagnetics* **18** 67–76
Korpinen L H, Elovaara J A and Kuisti H A 2009 Evaluation of current densities and total contact currents in occupational exposure at 400 kV substations and power lines *Bioelectromagnetics* **30** 231–40
Korpinen L H, Kuisti A K, Tarao H and Elovaara J A 2012 Occupational exposure to electric fields and currents associated with 110 kV substation tasks *Bioelectromagnetics* **33** 438–42
Leitgeb N and Cech R 2008 Dosimetric assessment of simultaneous exposure to ELF electric and magnetic fields *IEEE Trans. Biomed. Eng.* **55** 671–4
Santis V D, Chen X L, Cruciani S, Campi T and Feliziani M A 2016 Novel homogenization procedure to model the skin layers in LF numerical dosimetry *Phys. Med. Biol.* **61** 4428–37
Schmid G and Hirtl R 2016 On the importance of body posture and skin modeling with respect to *in situ* electric field strengths in magnetic field exposure scenarios *Phys. Med. Biol.* **61** 4390–4415
Shiau Y and Valentino A R 1981 ELF electric field coupling to dielectric spheroid models of biological objects *IEEE Trans. Biomed. Eng.* **28** 429–37
Stuchly M A and Dawson T W 2002 Human body exposure to power lines: relation of induced quantities to external magnetic fields *Health Phys.* **83** 333–40
Tarao H, Korpinen L, Kuisti H, Hayashi N, Elovaara J and Isaka K 2013 Numerical evaluation of currents induced in a worker by ELF non-uniform electric fields in high voltage substations and comparison of them with experimental results *Bioelectromagnetics* **34** 61–73
The European Parliament and the Council of the European Union 2013 Directive 2013/35/EU of the European parliament and of the council of 26 June 2013 on the minimum health and safety requirements regarding the exposure of workers to the risks arising from physical agents (electromagnetic fields) (20th individual Directive within the meaning of Article 16(1) of Directive 89/391/EEC) and repealing Directive 2004/40/EC *Official Journal of European Union* Directive 2013/35/EU
Yamazaki K, Kawamoto T, Fujinami H and Shigemitsu T 2005 Simplified dosimetry for human exposure to non-uniform ELF magnetic field *IEE Japan Trans. Fundam. Mater.* **125** 571–6
Yamazaki K, Kawamoto T, Fujinami H and Shigemitsu T 2007 On the method of investigating human exposure to nonuniform magnetic field *IEE Japan Trans. Fundam. Mater.* **127** 239–47